

# Comparison of SEVIRI Cloud Product with both the POLDER and the GLAS Space Lidar one

G. Sèze<sup>(1)</sup>, F. Parol<sup>(2)</sup>, J. Pelon<sup>(3)</sup>, C. Vanbauce<sup>(2)</sup>, H. Legleau<sup>(4)</sup>, M. Derrien<sup>(4)</sup>, M. Lalande<sup>(1)</sup>, J. Riedi<sup>(2)</sup>,  
and J.C. Buriez<sup>(2)</sup>

(1) *Laboratoire de Météorologie Dynamique, Université Pierre et Marie Curie, 75252 Paris Cedex 05, France.*  
*Email: seze@lmd.jussieu.fr*

(2) *Laboratoire d'Optique Atmosphérique, Université des Sciences et Technologies de Lille, 59655 Villeneuve d'Ascq  
Cedex, France*

(3) *Service d'Aéronomie, Université Pierre et Marie Curie, 75252 Paris Cedex 05, France*

(4) *Centre de Météorologie Spatiale Météo-France, BP 50547, 22307 Lannion Cedex, France.*

## ABSTRACT/RESUME

Cloud amount and cloud properties are key parameters of the climate system. They need to be adequately monitored. A promising way of improving cloud property retrieval is the combined use of new ensemble of data based on different measurement techniques. In the present study we focus on the comparison of cloud pressure distributions derived from four types of measurements: (1) the SEVIRI passive infrared measurements provided by the SAFNWC (Satellite Application Facility in support to NoW Casting), (2) spectral polarization measurements, and (3) absorption measurements in the oxygene A-band from the passive radiometer POLDER2 (POLarization and Directionality of the Earth's Reflectances) on board the ADEOS2 platform and (4) measurements from the space lidar GLAS (Geoscience Laser Altimeter System) on board the ICESAT platform. The October 2003 period is selected as both data from POLDER2 and GLAS are available at this period. The SAFNWC SEVIRI cloud top pressure, the POLDER Rayleigh cloud top pressure and the POLDER Oxygene cloud pressure distributions show the same global features and differences than those observed in a first SEVIRI/POLDER comparison for several days in June 2003. However, compared to the June 2003 results, for the October 2003 period, low cloud top pressure in the new version 1.2 of the SAFNWC SEVIRI products are closer to the POLDER Oxygene pressure. For high thick clouds, the SEVIRI and Rayleigh pressure are close. The more striking results of the preliminary comparison of the SEVIRI and space lidar GLAS cloud top pressure is that the cloud pressure distribution shapes are very similar over ocean as well as over land. As part of the A-train satellite constellation, PARASOL/POLDER has been launched in December 2004, the CALIPSO lidar and the CLOUDSAT radar have joined PARASOL and the A-Train in May 2006. Study of the relation between cloud properties observed from SEVIRI, POLDER and active measurements will be continued in this frame.

## 1. INTRODUCTION

Cloud amount and cloud properties are key parameters of the climate system. They need to be adequately monitored. Among the new generation of Earth-orbiting instruments designed for Earth's observation, the SEVIRI radiometer onboard Meteosat-8 provides high quality data with 3 km spatial resolution, 15 mn temporal sampling and 12 narrow spectral bands; the

POLDER radiometer launched on ADEOS-2 in December 2002 presents the particularity of having multispectral (8 solar spectral bands), multi-polarization and multi-directional (up to 14 different viewing angles) capabilities [1]. An overview of algorithms and products of the "Earth Radiation Budget, water vapor and clouds" line (hereafter "ERB & clouds") applied to POLDER data is presented in [2], [3] and [4]. POLDER2 "ERB & clouds" products are available from April 2003 to October 2003, the end of service of the ADEOS-2 platform. Six days in June 2003 were selected for comparison to preliminary SEVIRI output data of the SAFNWC (Satellite Application Facility in support to NoW Casting) cloud algorithm [5],[6]. On the other hand, a cloud classification based on a dynamical clustering method [7] was applied as an alternative method to SEVIRI radiance data provided by the Centre de Météorologie Spatiale (CMS) in Lannion (France). POLDER and SEVIRI cloud amount were compared and SEVIRI cloud type and cloud top pressure were checked against cloud pressure and thermodynamic phase retrieved from POLDER. Results of these comparisons were presented in [8].

In the present study we focus on the validity of cloud pressures derived from SEVIRI by the SAFNWC team. The October 2003 period is selected as data from the GLAS space lidar are also available at this period [9],[10]. Cloud top height and cloud layer structures provided by GLAS are used to help understanding the differences observed between the SEVIRI cloud pressures and the POLDER ones [8]. Section 2 presents a short description of the cloud parameters (pressure and cloud type) compared in this study. In section 3, SEVIRI cloud top pressure are checked against cloud pressure and thermodynamic phase retrieved from POLDER; quantitative comparison with results discussed in [8] but for June 2003 is presented. GLAS measurements, available for October 2003 but not coincident with POLDER overpass times, are compared to the SEVIRI cloud top pressure and cloud type in section 4. Conclusions and perspectives are given in section 5.

## 2. BRIEF DESCRIPTION OF THE CLOUD PROPERTY RETRIEVALS.

### 2.1 The SAFNWC SEVIRI cloud type and cloud top pressure retrievals

Presently, the SAFNWC provides cloud mask, cloud type and cloud top temperature/pressure/height maps, by using the multi-spectral capabilities of the SEVIRI radiometer [11], [6]. In the future, cloud top phase maps will be added to the cloud products. The first stage in the SAFNWC cloud product derivation is the sorting between cloud free and cloud contaminated pixels. It is based on a serie of sequential threshold tests. The process is stopped if one test is successful. The test that allows the cloud detection is stored and a quality flag is computed.

The main interest of the cloud type product developed within the SAFNWC framework is to provide a detailed cloud analysis to support nowcasting applications. Using spectral and textural features, cloudy pixels are classified first in two sets: (1) fractionnal and high semitransparent cloud, (2) low, medium and high thick. The separation between fractionnal, high semitransparent cloud and high semitransparent cloud over low or medium cloud is performed using spectral features. For thick cloud, the separation in very low cloud, low cloud, medium cloud, high cloud and very high cloud is performed using Numerical Weather Prediction (NWP) forecast temperature.

The cloud top pressure is retrieved from the 10.8  $\mu\text{m}$  brightness temperature for low, medium and thick clouds. For high thin clouds, a correction for semi-transparency is applied using two infrared channels, a window (10.8  $\mu\text{m}$ ) channel and a sounding (13.4  $\mu\text{m}$ , 7.3  $\mu\text{m}$  or 6.2  $\mu\text{m}$ ) one. For fractional clouds, the top pressure is not estimated.

The first set of data (June 2003) provided by the CMS and used in the first comparison of SEVIRI and POLDER [8] was from the product version 1.0 [11]. The product version of the data set coincident used in this study is 1.2 [12]. The major change between the two versions relates the estimation of the low cloud pressure in case of thermal inversion in the NWP forecast air temperature vertical profile at low level. This change tends to place the cloud top level under the low level inversion, e.g. at a lower pressure level. Results of a comparison of the cloud top pressure product version 1.2 with radio-sounding data and with ground based radar and lidar data are given in [13].

## 2.2 The POLDER cloud property retrievals

The POLDER cloud amount is determined by applying first a cloud detection algorithm to each full-resolution pixel (6.2 km x 6.2 km) and for every viewing direction. Then the cloud cover is computed at the super-pixel scale (3 x 3 pixels) and a quality index is defined from concurrent responses to the different tests. See [2],[3] for a complete description of this algorithm.

For cloudy super-pixels, an algorithm for remotely determining the cloud-top thermodynamic phase is applied. The algorithm utilizes near-infrared polarized reflectance over a large range of scattering angles in order to discriminate between ice and liquid water

phases [4],[14]. Indeed, theoretical as well as experimental studies have shown that polarized signatures of water droplets and ice particles are quite different. The last version of the algorithm has been applied to the data used in this study. Compared to the version of the algorithm used for the June 2003 data set [8], this improved version uses more strict conditions in particular on the range of scattering angle required to estimate the phase. If this conditions are not met, a cloud phase is attributed from a rough estimation of the pressure. A quality index is attached to the cloud phase product.

For cloudy super pixels with optical thickness above 3, two different methods were developed to retrieve cloud pressure. The first one is derived from absorption measurements in the oxygen A-band and the second one is derived from spectral polarization measurements. The derivation of the "Oxygen pressure"  $P_{\text{oxy}}$  is based on a differential absorption technique using the radiances measured in the POLDER narrowband and wideband channels centred on the oxygen A-band. [15] have shown that  $P_{\text{oxy}}$  is found to be close to the mean pressure of clouds when compared to ARM/MMCR cloud boundary pressures. Another retrieved cloud pressure is the so-called "Rayleigh cloud pressure",  $P_{\text{Ray}}$ , derived from polarization measurements at 443 nm [3]. At this wavelength, the polarized reflectance is mainly related to the atmospheric molecular optical thickness above the observed cloud, at least for scattering angles ranging from 80° to 120° and outside the sunglint direction. That pressure is thus expected to be close to the cloud top pressure.

## 2.3. The GLAS cloud layer retrieval

The spaceborne lidar measurements are made under the track of the satellite using two channels, one operating at 532nm and the other at 1064nm. The swath is very narrow. The laser pulse rate of 40Hz, yields vertical profiles at approximately 172m spacing along a given orbit track with a vertical resolution of 76.8m. A list of the GLAS data products is given in [10], [16]. The cloud layer boundaries (GLA09) are determined from the calibrated, attenuated backscatter cross sections (GLA07). For the cloud to be detected, the attenuated backscatter cross section must be larger than a given threshold on the signal-to-noise ratio reachable for a given horizontal-vertical resolution. During the October 2003 period, the 532 nm channel was more sensitive and has been used to determine cloud layers.

Cloud top heights from 532 nm are determined at four different sampling rates (horizontal resolution) in the following order: 4 s, 1 s, 0.2 s, and 0.25 s [16]. If a cloud layer height is found at 4 s time interval, then a search is performed at 1 s and so on down to the smallest time interval. In the present study, results at 1s time interval (about 7 km horizontal resolution) have been used.

Another useful parameter given in the GLA09 product is the presence or absence of a surface echo. This

parameter allows to separate scenes completely covered by opaque clouds from scenes covered by thin or broken cloud layers. In the GLA09 product, not only the heights but also the pressure levels at top and base of detected cloud layers are given.

## 2.4 Selected data set

POLDER2 “ERB & Clouds” products are available for the April to October 2003 period. The initial on-orbit full operation of the GLAS instrument began on September 28, 2003 until November 18, 2003. For 86 GLAS orbits and 65 POLDER orbits distributed over 17 days in September-October 2003, (although the SEVIRI calibration was not final) the SAFNWC provided the SEVIRI radiance fields and its cloud products coincident in time with the GLAS or the POLDER overpasses. For GLAS, the time of the descending/ascending node is 7:30/19:30 and for POLDER, the time of the descending node is 10:30. Thanks to the 15' repeat cycle of Meteosat-8/SEVIRI, the time-lag is at the most of 7.5' between the SEVIRI and GLAS or the SEVIRI and POLDER coincident data sets.

POLDER “ERB & Clouds” products (final product at 18.5 km x 18.5 km resolution) and the 1s. GLAS cloud layer product (7.5km horizontal resolution) have been projected on the SEVIRI grid (3.3 km x 3.3 km at sub-satellite point).

## 3. POLDER AND SEVIRI CLOUD PRESSURES IN OCTOBER 2003

Figure 1 displays the SAFNWC cloud top pressure (Fig. 1a), the POLDER Rayleigh cloud top pressure (Fig. 1b), the POLDER Oxygen cloud pressure (Fig. 1c) and the POLDER cloud phase (Fig. 1d) retrieved for the October 20, 2003. The three cloud pressure maps, are in agreement with what has been presented in our previous paper on the comparison of SEVIRI and POLDER cloud properties [8]. The main characteristics of the two cloud top pressure maps (SEVIRI and POLDER Rayleigh pressure) are coherent with that found in the analysis of the SEVIRI cloud type maps (not shown) and POLDER cloud phase maps. As expected, the POLDER oxygen cloud pressure is on average higher than the cloud top pressures (see for example the stratocumulus cloud deck in the south part of the Atlantic ocean). If the main characteristics of the two cloud top pressure maps are coherent, some differences are however observed between them (see fig 1.a and fig1.b). Pressure of low clouds is higher in the SEVIRI results than in the Rayleigh map. Some very low pressure values (high clouds) appear in the Rayleigh map.

The distributions and average values of the 3 cloud top pressures over ocean and over land are reported in Figure 2 and table 1. The shapes of these distributions obtained for 15 days in October 2003 are similar to those obtained for the 6 days of June 2003 already discussed in [8]. However, over ocean, the high pressure

peak of the SEVIRI distribution is shifted towards higher pressure value while the high pressure peak of the Rayleigh distribution is shifted towards lower pressure value. Both over ocean and over land, very low Rayleigh pressure values are observed in October; this is not the case in the SEVIRI cloud pressure distribution.

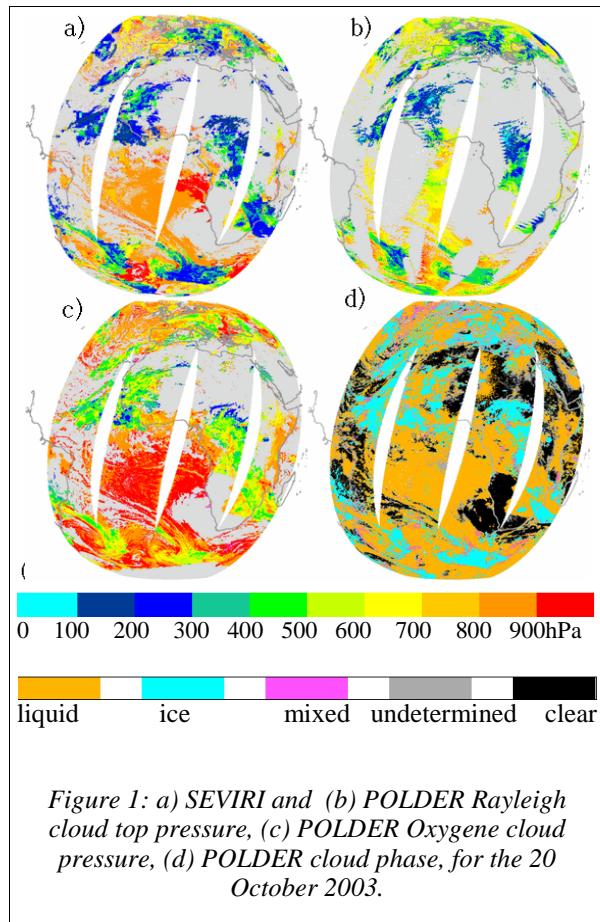


Figure 1: a) SEVIRI and (b) POLDER Rayleigh cloud top pressure, (c) POLDER Oxygen cloud pressure, (d) POLDER cloud phase, for the 20 October 2003.

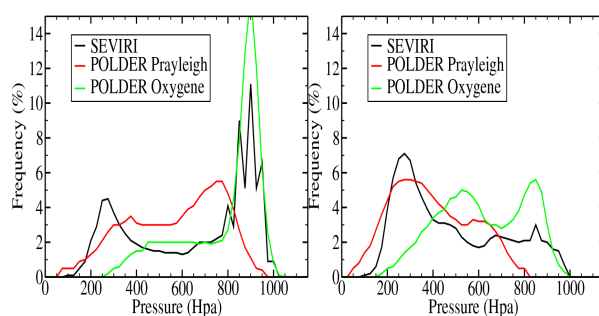


Figure 2: Cloud pressure distributions over ocean (left) and over land (right) for 15 days of October, 2003.

For the 3 cloud pressure distributions and for June and October over ocean and land, the average pressure as a function of cloud phase is given in table 2. When comparing June and October 2003, SEVIRI and Rayleigh pressure mean values for liquid clouds vary in an opposite manner. This is observed over ocean (Table 2) as well as over land (results not shown). On the average for ice clouds the SEVIRI pressure values remain the lowest.

The changes observed in the cloud pressure

distributions between the June and October data set are coherent with the changes performed in the SAFNWC algorithm for the estimation of low cloud pressure (see section 2.1 and 2.2).

Table1: SAFNWC, Rayleigh and Oxygene mean pressures in hPa for the October and June 2003 cases.

	Ocean			Land		
	SEV	Ray.	Oxy.	SEV	Ray.	Oxy.
Oct.	638	572	775	492	432	651
June	594	616	751	502	500	671

Table2: Average pressures in hPa for the October and June cases over ocean and land in function of POLDER cloud phase.

	Liquid			Ice		
	SEV.	Ray.	Oxy.	SEV.	Ray.	Oxy.
Oct.	685	593	809	331	357	525
June	635	640	786	350	403	538

#### 4. GLAS AND SEVIRI

An example of simultaneous SEVIRI pressure fields and GLAS cloud layer profile is given in figure 3 for two cases on October 10, 2003. A high cloud system over west Africa is observed in the first case and a thick low cloud deck in the subsidence region offshore Namibia in the second profile.

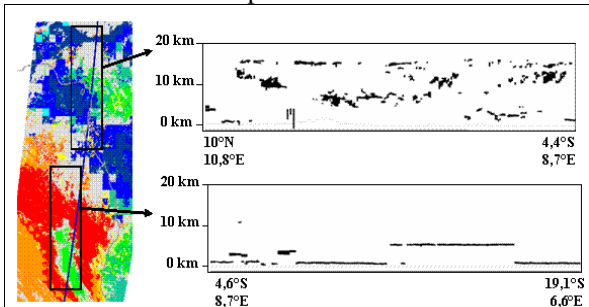


Figure 3: SEVIRI cloud top pressure and coincident GLAS cloud layers for two cases along a GLAS orbit on October 10, 2003.

##### 4.1 GLAS and SEVIRI cloud types

The classification of GLAS cloudy column in cloud types is performed according to three criteria. The first criterion is the pressure of the highest layer. The atmospheric column is divided in ten levels of pressure. The second criterion discriminates thin/broken cloud scene from thick cloud scene using the surface echo flag. The third criterion classifies the cloudy columns in single layer and multi-layer cloud scene. The single layer case corresponds to cases for which clouds are gathered in only one of the ten pressure levels. The

multi-layer case corresponds to the other cases. In this classification, high clouds correspond to cloudy column with a cloud top pressure below 400hPa, medium correspond to cloudy column with a cloud top level between 400hPa and 700hPa and low clouds correspond to cloudy column with a cloud top pressure larger than 700hPa.

In the SAFNWC SEVIRI cloud type classification 10 cloud classes are defined: partial, very low, low, middle, thick high, very thick high, very thin cirrus, thin cirrus, cirrus, cirrus over.

In a first step of the analysis, SEVIRI cloud types as well as GLAS ones are merged into 4 main types, clear and low, middle, high clouds. It is found that over ocean/land for the 86 GLAS studied orbits distributed over 17 days in September-October 2003, 74%/72% of pixels fall in the same class. The pixels corresponding to the SAFNWC partial cloud class have been excluded of the comparison (16%/4% of the total).

The distribution of the 4 GLAS main cloud types has been studied for each SEVIRI cloud class. To this respect, the 10 SEVIRI cloud types have been gathered in 6 cloud types, clear, partial cloud cover, low, middle and high cloud, cirrus over another layer (called "cirrus over"). Results are reported in Figure 4. Over ocean as well as over land, for the SEVIRI high cloud type, GLAS has effectively detected a high cloud layer in more than 85% of the cases; for the SEVIRI "cirrus over" class, this percentage reaches 70%.

If the SEVIRI low cloud type is consistent with the GLAS classification in 75% of the cases over ocean, over land the percentage drops to only 45% of the cases. Both over ocean and over land for the SEVIRI middle cloud class the percentage of agreement with GLAS classification is less than 60%. Pixels classified in the SEVIRI partial cloud class do not belong to a well defined GLAS cloud class.

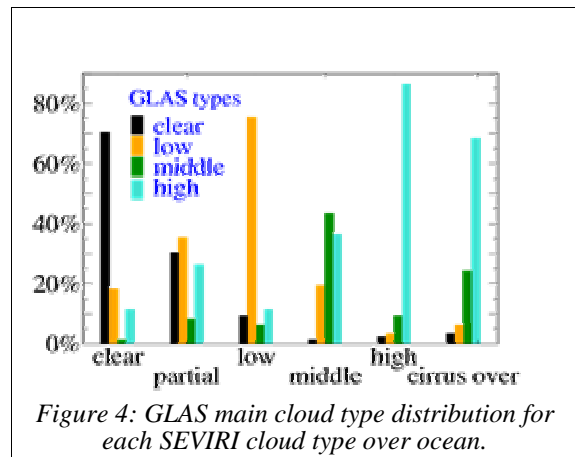


Figure 4: GLAS main cloud type distribution for each SEVIRI cloud type over ocean.

##### 4.2 GLAS and SEVIRI cloud pressure

In this section we define the parameter "GLAS cloud pressure" as the top pressure of the highest cloud layer detected by GLAS.

For the 86 GLAS orbits distributed over 17 days in September and October 2003, the global shapes of the SEVIRI and GLAS cloud pressure distributions are "remarkably" similar (see Fig. 5). Over ocean the

distributions present two peaks with a strong decrease between 400 and 700hPa. Over land there is only one peak at low pressure values and a relatively uniform distribution between 500 and 850hPa over land. However, a bias towards higher pressure values appears in the SEVIRI curves compared to the GLAS ones.

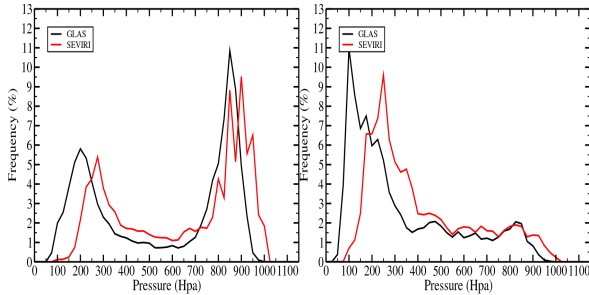


Figure 5: GLAS and SEVIRI cloud pressure distributions over ocean (left) and over land (right)

The bidimensional distribution of the two cloud pressures (not shown) indicates a good correlation between the two set of pressures and confirms the bias observed in figure 5 especially for high clouds. The mean difference between the SEVIRI and GLAS pressures is 67hPa and the RMS is 180hPa.

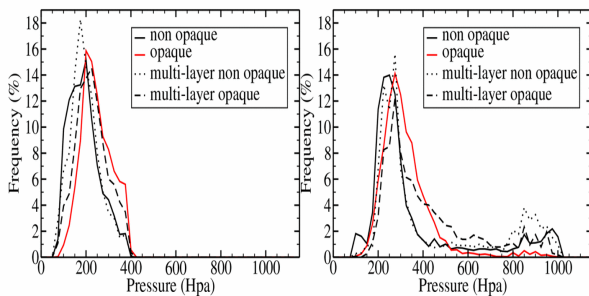


Figure 6: GLAS (left) and SEVIRI (right) cloud top distributions for the four GLAS high cloud classes over ocean.

Figure 6 shows the GLAS (left) and SEVIRI (right) cloud top distributions for the four GLAS high cloud types over ocean. For GLAS the non opaque curve presents the largest percentage of very low pressure. For the opaque case, we find more pressure values close to the 400hPa boundary (defined as the boundary for the high cloud type in the GLAS algorithm).

This is also the case for the SEVIRI pressure (right) for the GLAS opaque cloud classes. A non negligible percentage of cloud top pressure above 400hPa is found in the SEVIRI distributions, excepted for the opaque single layer curve.

It is for middle level clouds that the largest differences are found between the GLAS and SEVIRI cloud pressure distributions (not shown). For GLAS non opaque middle cloud type the SEVIRI pressures values are almost equitably distributed between 200 and 1000hPa. “Surprisingly”, for opaque clouds, there are SEVIRI cloud top pressures below 400hPa.

A sub-classification of the GLAS low cloud depending on the cloud top pressure of the highest layer is performed. Over land and for the opaque GLAS single-

layered low cloud class, the SEVIRI cloud pressures are split in three sub-classes (cloud top pressure (1) between 700 and 850hPa, (2) between 850 and 925hPa and (3) above 925hPa). The results are shown in figure 7. The three distributions obtained for SEVIRI move in agreement with the increase in the values of cloud pressures retained for GLAS. The percentage of pressure values below 600hPa is very small. Over ocean (not shown) distribution shapes are more peaked and very low pressure values are almost absent.

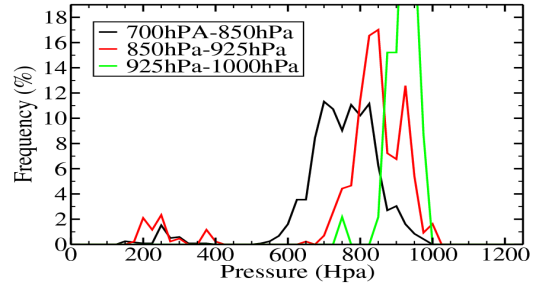


Figure 7: SEVIRI cloud pressure distribution for GLAS opaque single layer low clouds over land.

Table3 gives the mean differences between the SEVIRI and GLAS cloud top pressure and the RMS of the differences for the 3 main cloud types: high, middle and low clouds. Table 4 is equivalent to table 3 but for the single-layered opaque cloud case. A strong decrease in the mean and RMS differences is observed for high cloud when only the single-layered opaque cases are taken into account.

Table3: SEVIRI minus GLAS cloud top differences for GLAS high, middle and low clouds.

	<i>Ocean</i>		<i>Land</i>	
	Mean	Rms	Mean	Rms
High	148hPa	249hPa	104hPa	169hPa
Middle	42hPa	161hPa	-6hPa	119hPa
Low	5hPa	96hPa	-38hPa	135hPa

Table4: SEVIRI minus GLAS cloud top differences for GLAS high, middle and low single layer opaque cloud

	<i>Ocean</i>		<i>Land</i>	
	Mean	Rms	Mean	Rms
High	58hPa	99hPa	50hPa	92hPa
Middle	3hPa	123hPa	-21hPa	101hPa
Low	0.5hPa	93hPa	50hPa	140hPa

For the low level cloud over land, there is a bias of 50hPa when only single-layered opaque case is taken into account.

## 5. CONCLUSION AND PERSPECTIVES

Cloud pressure distributions derived from SEVIRI by

the SAFNWC team have been compared with the POLDER Rayleigh cloud top pressure and the Oxygene cloud pressure for several days in October 2003. These distributions show the same global features and differences than those observed in the first SEVIRI/POLDER cloud pressure comparison operated for several days in June 2003 [4].

However, for low cloud over ocean when comparing June and October 2003 there is a decrease of the Rayleigh pressures and an increase of the SEVIRI pressures. The SEVIRI cloud pressures increase according to the change in algorithm version from 1.0 to 1.2. In October over ocean, the SEVIRI low cloud top pressure is very close to the Oxygene cloud pressure. However, at the present time the Rayleigh pressure increase is not well explained.

For high thick clouds, the SEVIRI and Rayleigh cloud pressures are close and for high thin clouds the SEVIRI pressure is smaller than the Rayleigh one. In October 2003, some very low cloud pressure values are retrieved from the Rayleigh method whereas there were not present in June 2003.

For the same days in October 2003 SEVIRI cloud top pressure has been compared with the cloud top pressure of the highest layer observed with the space lidar GLAS. Unfortunately, accounting for the different overpass times, GLAS and POLDER data are not coincident. Both over ocean and over land the SEVIRI and GLAS pressure distribution shapes are very similar. There is a bias of 67hPa towards higher pressure values for the SEVIRI pressure compared to the GLAS pressure. 62% of the GLAS high clouds are classified high clouds by SEVIRI. For the GLAS single layer opaque high cloud, the bias between the SEVIRI and GLAS cloud top pressure is below 58hPa.

The GLAS middle cloud class does not correspond to a well defined level pressure in the SEVIRI data set. A more precise comparison must be performed to understand this behaviour, in particular the non negligible percentage of low SEVIRI cloud pressure.

Over ocean, for the GLAS low clouds when SEVIRI detects also clouds, the mean difference between the SEVIRI and GLAS cloud top pressure is almost zero but the RMS is close from 95hPa. Over land, more than 55% of SEVIRI low clouds are equally distributed in the clear, middle and high cloud GLAS classes.

As part of the A-train satellite constellation, PARASOL/POLDER has been launched in December 2004, the CALIPSO lidar and the CLOUDSAT radar have joined PARASOL and the A-Train in May 2006. Study of the relation between cloud properties observed from SEVIRI, POLDER and active measurements will be continued in this frame.

## 6. REFERENCES

1. Deschamps, P. Y., F. M. Bréon, M. Leroy, A. Podaire, A. Bricaud, J. C. Buriez, and G. Sèze: The POLDER mission: Instrument characteristics and scientific objectives. *IEEE Trans. Geosci. Rem. Sens.*, **32**, 598-615, 1994.

2. Buriez, J. C., C. Vanbauce, F. Parol, P. Goloub, M. Herman, B. Bonnel, Y. Fouquart, P. Couvert, and G. Sèze: Cloud detection and derivation of cloud properties from POLDER. *Int. J. Remote Sensing*, **18**, 2785-2813, 1997.
3. Parol, F., J.C. Buriez, C. Vanbauce, P. Couvert, G. Sèze, P. Goloub, and S. Cheinet: Information Content on Clouds from ADEOS-POLDER. *IEEE Trans. Geosci. Remote Sens.*, **37**, 1597-1612, 1999.
4. Parol F., J.C. Buriez, , C. Vanbauce, J. Riedi, L. C.-Labonnote, M. Doutriaux-Boucher, M. Vesperini, G. Sèze, P. Couvert, M. Viollier, and F.M. Bréon: Review of capabilities of multi-angle and polarization cloud measurements from POLDER, *Adv. Space Res.*, **33**, 1080 -1088, 2004.
5. Derrien, M. and H. Le Gléau, 2005, MSG/SEVIRI cloud mask and type from SAFNWC. *International Journal of Remote Sensing*, **26**, 4707-4732.
6. Derrien, M. and H. Le Gléau, SAFNWC/MSG SEVIRI Cloud Product, Proceeding of the EUMETSAT Meteorological Satellite Conference, 191-198, 2003.
7. Sèze, G. and H. Pawlowska: Cloud Cover Analysis with METEOSAT-5 during INDOEX, *J. Geophys. Res.*, **D22**, 28,415, 2001.
8. Sèze, G., F.Parol, J.C. Buriez, P. Couvert, M. Doutriaux-Boucher, H. Le Gléau, J. Riedi and C. Vanbauce: Comparison of cloud types observed from SEVIRI and POLDER2. ESA SP-582., 73-77, Proc Second MSG workshop. Salzburg, 9-10 September 2004.
9. Schutz B.E., H.J. Zwally, C.A. Shuman, D. Hancock and J.P. DiMarzio: Overview of the ICESat Mission. *Geophys. Res. Lett.*, **32**, L21S01, doi:10.1029/2005GL0240009, 2005.
10. Spinhirne, J.D., S.P. Palm, W.D. Hart, D.L. and E.J. Welton 2005: Cloud and Aerosol measurements from GLAS: Overview and initial results, *Geophys. Res. Lett.*, **32**, L22S03, doi:10.1029/2005GL023507.
11. User Manual for the PGE01-02-03 of the SAFNWC/MSG: Scientific Part. To be downloaded from [www.meteorologie.eu.org/safnwc](http://www.meteorologie.eu.org/safnwc)
12. Scientific report an Additional Tuning of MSG PGE01-02-03 following validation activities. To be downloaded from [www.meteorologie.eu.org/safnwc](http://www.meteorologie.eu.org/safnwc)
13. Derrien, M., H. Le Gléau, J.F.Daloze, M.Haefelin, 2005: Validation of SAFNWC/MSG cloud products with one year of SEVIRI data. Proceeding of the 2005 EUMETSAT Meteorological Satellite Conference, 95-103.
14. Riedi, J., M. Doutriaux-Boucher, P. Gloub, P. Couvert: Global Distribution of Cloud Top Phase from POLDER/ADEOS1. *Geophys. Res. Lett.*, **28**,1707-1710,2000.
15. Vanbauce, C., B. Cadet, and R.T. Marchand: Comparison of POLDER apparent and corrected oxygen pressure to ARM/MMCR cloud boundary pressures. *Geophys. Res. Lett.*, **30** (5), 1212, doi:10.1029/2002GL016449, 2003.
16. Palm, S., W.Hart, D. Hlavka, E.J. Welton, A. Mahesh, and J. Spinhirne 2002: Geoscience Laser Altimeter System (GLAS) atmospheric data products, algorithm theoretical basis document, version 4.2, pp 137, NASA Goddard Space Flight Center, Greenbelt, Md.